Boletim Técnico da Escola Politécnica da USP

Departamento de Engenharia Eletrônica

ISSN 1413-2206

BT/PEE/9908

H_2 and H_∞ Control for MagLev Vehicles

Anselmo Bittar

Roberto Moura Sales

São Paulo – 1999

O presente trabalho é um resumo da tese de doutorado apresentada por Anselmo Bittar, sob orientação do Prof. Dr. Roberto Moura Sales.: "Controle da Suspensão Eletromagnética do Protótipo de um Veículo", defendida em 07/07/98, na Escola Politécnica.

A íntegra da tese encontra-se à disposição com o autor e na Biblioteca de Engenharia de Eletricidade da Escola Politécnica/USP.

FICHA CATALOGRÁFICA

Bittar, Anselmo
'H IND.2'and H 'INFINITE' control for MagLev vehicles / A. Bittar, R.M. Sales. -- São Paulo : EPUSP, 1999.
p. -- (Boletim Técnico da Escola Politécnica da USP, Departamento de Engenharia Eletrônica, BT/PEE/9908)

1. Veículos levitados 2. Levitação magnética I. Sales, Roberto Moura II. Universidade de São Paulo. Escola Politécnica. Departamento de Engenharia Eletrônica III. Título IV. Série
ISSN 1413-2206 CDD 388.44
538.3

H_2 and H_∞ Control for MagLev Vehicles

Anselmo Bittar and Roberto Moura Sales

In recent years, many magnetically levitated transport systems have been constructed, tested, and improved. Various magnetic levitation (MagLev) system technologies are being developed, and some of them, including the prototype featured in this article, use electromagnets for vehicle levitation. Vehicle levitation is achieved by controlling the gaps of these electromagnets.

The constructed prototype will have independent levitation and propulsion systems, but the focus of this article is on the levitation system only. The system is open-loop unstable, highly nonlinear, and it has a very restricted equilibrium region. A Single Input Single Output (SISO) analytical model and closed-loop identification experiments are presented, with emphasis on design procedures of H_2 and H_∞ controllers applied to the electromagnetic levitation system. For the designs of these controllers, a special choice of weighting functions is employed to attenuate the resonance peak at low frequencies in the closed-loop system. The results show that closed-loop system responses with H_2 and H_∞ controllers are very similar and present better performances when compared to the response obtained with a classical controller.

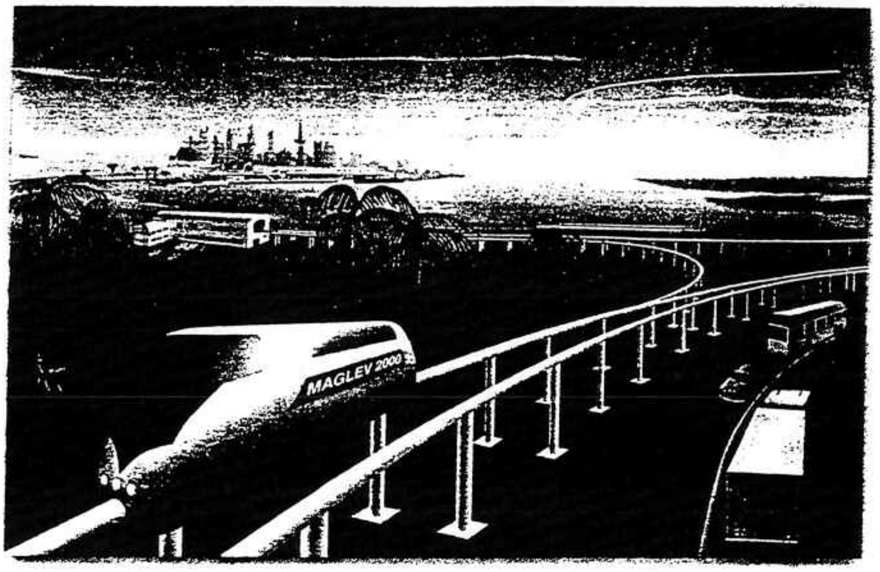

Magnetic Levitation Transport Systems

New MagLev transport systems are being researched around the world. The vehicles are magnetically levitated, and their guide and propulsion forces are also generated magnetically. Due to the absence of contact friction, this kind of vehicle can reach high speeds easily.

MagLev systems have several advantages when compared to traditional railway systems in that the absence of contact reduces noise, component wear, vibrations, maintenance costs, etc. MagLev vehicles are better able to climb steep ramps and tolerate curves with smaller radii. Smaller radii and higher superelevation coefficients allow the construction of shorter guideways that are more economical [1].

Basically, three kinds of technologies for MagLev vehicles have been developed [1]:

- Permanent magnetic: The levitation system provided by permanent magnets uses repulsive magnetic forces. Until now, this line of development has not been economical.
- Electrodynamic: The electrodynamic system works through repulsive forces, too, but uses superconducting materials to generate the forces. A vehicle with this kind of suspension presents some disadvantages [2]: at high speeds, the damping forces are weak, and, at low speeds, the levitation force is weak and the braking force is strong. Thus, levitation is feasible only at high speeds.
- Electromagnetic: In an electromagnetic levitation system, the vehicle is levitated through attractive forces produced by electromagnets. It is simpler than the electrodynamic system, in the sense that it does not need a cooling system for the superconducting coils. Another advantage is that it can be levitated equally at any speed, since the attractive force is independent of the speed. On the other hand, such a system is unstable and strongly nonlinear, with a severely restricted equilibrium region, which makes it difficult to obtain closed-loop stability.

Various prototypes have been constructed, tested, and improved for MagLev transport systems [3]–[11].

This article is an expanded version of a paper that appeared in the Proceedings of the 1997 IEEE International Conference on Control Applications. This work was supported by FAPESP (Sao Paulo State Research Council) under grant 95/6968-7. *The authors are with the Electronic Engineering Department, University of Sao Paulo, Av. Prof. Luciano Gualberto, trav. 3, n. 158, CEP 05508-900, Brazil, (anselmo, roberto)@lac.usp.br.*

 0272-1708/98/$10.00©1998IEEE

System Description

The prototype system (Fig. 1) featured in this article is basically a vehicle that has independent electromagnets that, through gap control, lift it on an elevated guideway.

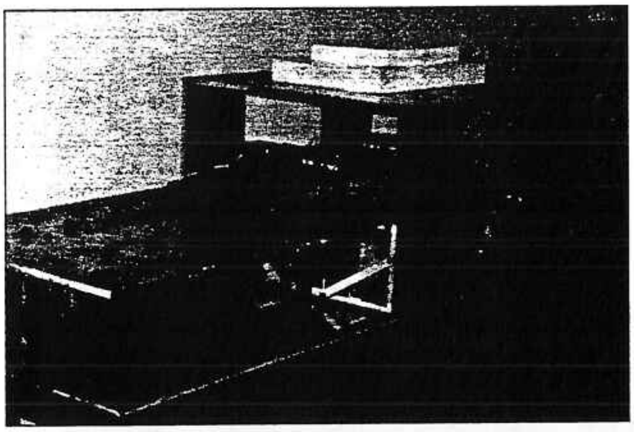

Fig. 1. Electromagnetically levitated vehicle prototype.

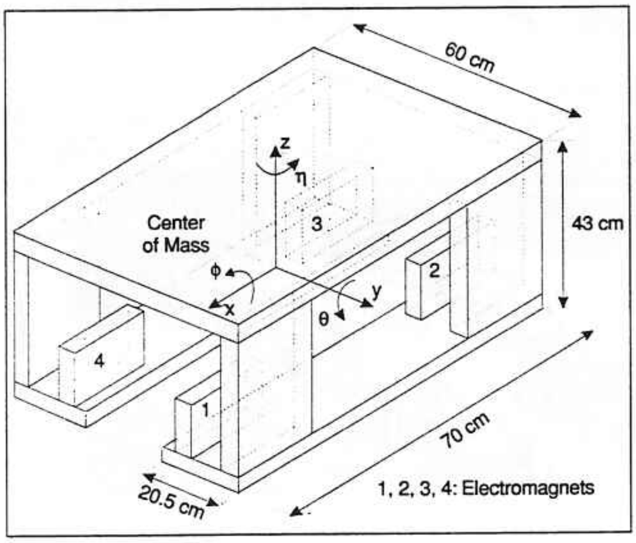

Fig. 2. Vehicle and electromagnets.

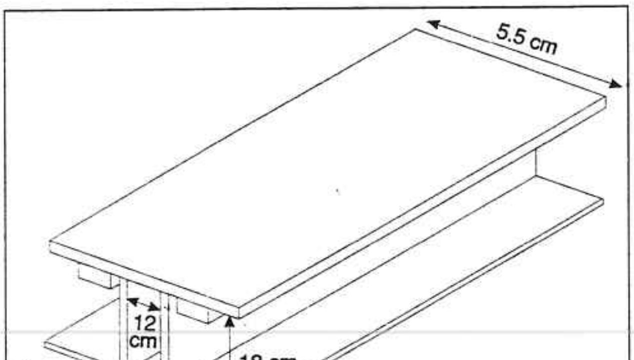

Fig. 3. Elevated guideway.

Vehicle and Guideway

Levitation in the prototype system is achieved by attractive forces developed by four electromagnets that were positioned in each extremity of the vehicle, as shown in Fig. 2. There are also four gap sensors to measure the gaps of these electromagnets. The magnetic forces developed by electromagnets are always attractive forces (whichever the magnetic flux direction), and an elevated guideway is also necessary (Fig. 3). A frontal view of the vehicle in the levitation state in the elevated guideway is presented in Fig. 4. Vehicle levitation is performed through SISO controls of each gap z_p $(p = 1, \ldots, 4)$.

The vehicle has six degrees of freedom, which correspond to the three translation motions (surge $x(t)$, sway $y(t)$, and heave $z(t)$) and to the three rotation motions (roll $\phi(t)$, pitch $\theta(t)$, and yaw $\eta(t)$). The vehicle will have independent lift, guide, and propulsion systems, but only the levitation system ($z(t)$, $\phi(t)$, and $\theta(t)$) is considered in this article. In order to control the guide system ($y(t)$ and $\eta(t)$), it is necessary to use four additional lateral electromagnets and to control the respective gaps.

The vehicle is constructed with aluminum plates. The guideway through which the magnetic flux flows is constructed with thin iron bars. Laminated guideways would be an alternative choice in order to reduce eddy currents, which produce drag and repulsive forces. Drag forces cause power loss, and repulsive forces reduce the lift forces [12]. However, iron bars were employed to simulate problems that will certainly be present in any real system.

Table 1 presents some prototype characteristics.

Electromagnets for Levitation

The prototype has independent electromagnets to lift the vehicle. This kind of construction provides controllers with simpler structures and improves the reliability of the system. The levitation electromagnets have an "E" shape as shown in Fig. 5. For this type of electromagnet, the attractive force is given by

$$F(t) = k_f \left(\frac{i(t)}{z(t)} \right)^2, \tag{1}$$

where $i(t)$ is the input electrical current, $z(t)$ is the output air gap, and $k_f = \mu_0 acN^2 / 2$ is a constant. It is important to mention that

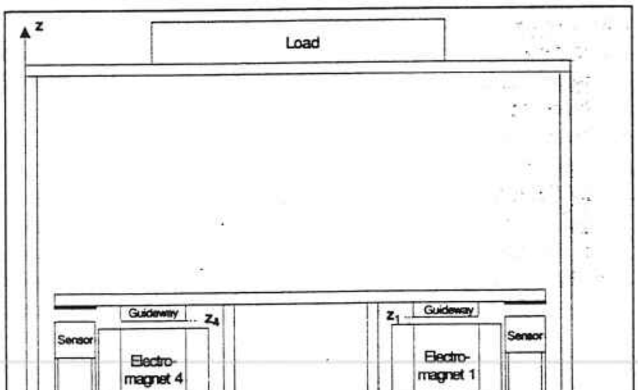

Fig. 4. Frontal view of the vehicle in the levitation state.

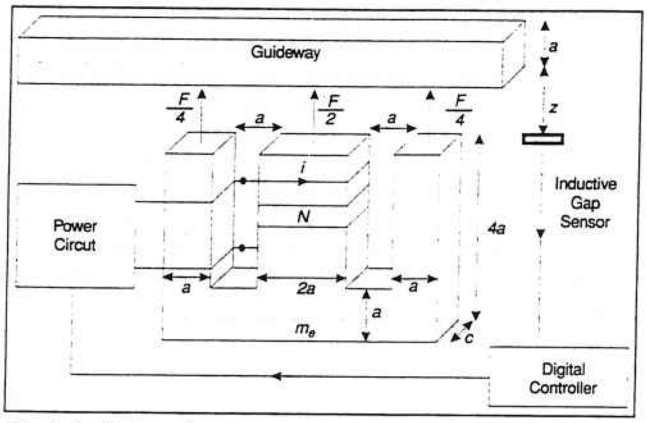

Fig. 5. Levitation electromagnet.

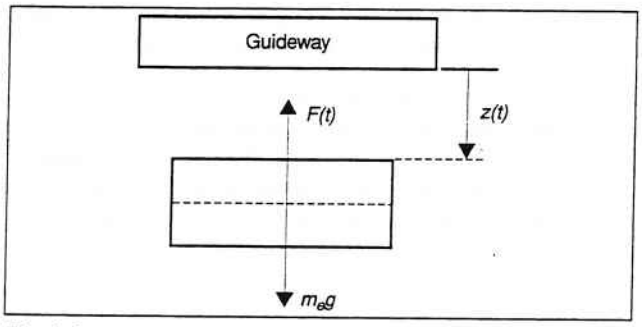

Fig. 6. System representation for a quarter section of the vehicle.

Table 1. Prototype characteristics	
Length	70 cm
Width	60 cm
Height	43 cm
Mass	$M = 97.6$ kg
Supply voltage	55 V dc
Levitation power	377 W

Equation 1 is valid for $z(t) > z_{sat}$ only, where $z_{sat} > 0$ is the smallest gap for which magnetic nucleus saturation does not occur.

Qualitatively, the choice of the steady-state gap is directly related to opposite requirements of energy consumption and levitation system robustness. In terms of energy consumption, it would be interesting to set the gap as small as possible, because the current necessary to levitate the vehicle would be smaller than the current for higher gaps. However, for very small gaps, the coil inductance becomes higher, making a faster control action difficult. Therefore, to obtain better levitation system robustness, it would be necessary to set higher gaps, since the coil inductance is smaller. The prototype's nominal gap is set as $Z_0 = 5$ mm. This choice also depends on the total mass of the vehicle and electromagnet dimensions.

System Modeling

A mathematical model for the vehicle was developed. Due to the use of various electromagnets in a real application [9] and considering constructive differences, an overall control system constituted of SISO controllers is simpler and more easily tuned. Thus, the vehicle is modeled by four decoupled SISO systems.

Fig. 6 shows a system representation for a quarter section of the vehicle. In this figure, m_e represents a quarter of the vehicle total mass. The nonlinear differential equation that represents the system shown in Fig. 6 is given by

$$m_e\ddot{z}(t) = m_e g - F(t) = m_e g - k_f\left(\frac{i(t)}{z(t)}\right)^2, \tag{2}$$

where g is the local gravity acceleration.

Supposing small disturbances $\Delta Z(t)$ and $\Delta I(t)$ around the equilibrium point (I_0, Z_0), the linearization of Equation 2 gives

$$m_e\Delta\ddot{Z}(t) = k_z\Delta Z(t) - k_i\Delta I(t), \tag{3}$$

where

$$k_z = \frac{2k_f I_0^2}{Z_0^3} \text{ and } k_i = \frac{2k_f I_0}{Z_0^2}.$$

At the equilibrium point (I_0, Z_0), Equation 2 produces

$$I_0 = Z_0\sqrt{\frac{m_e g}{k_f}}. \tag{4}$$

From Equations 3 and 4,

$$\Delta\ddot{Z}(t) = \frac{2g}{Z_0}\Delta Z(t) + \frac{2g}{I_0 k_{pot}}\Delta V(t), \tag{5}$$

where the power circuit dynamics are approximated by a constant $k_{pot} > 0$, with $\Delta V(t) = -k_{pot}\Delta I(t)$.

Considering that $\Delta Z(t) = k_s\Delta Z_\upsilon(t)$, where $\Delta Z_\upsilon(t)$ is the gap measured in volts and k_s is the sensor gain, Equation 5 yields:

$$\Delta\ddot{Z}_\upsilon(t) = \frac{2g}{Z_0}\Delta Z_\upsilon(t) + \frac{2g}{I_0 k_{pc}}\Delta V(t), \tag{6}$$

where $k_{pc} = k_s k_{pot}$.

From Equation 6, the following open-loop system transfer function is obtained:

$$G(s) = \frac{\Delta Z_\upsilon(s)}{\Delta V(s)} = \frac{\frac{2g}{I_0 k_{pc}}}{\left(s + \sqrt{\frac{2g}{Z_0}}\right)\left(s - \sqrt{\frac{2g}{Z_0}}\right)}. \tag{7}$$

Table 2 presents some design data for each electromagnet.

In order to validate the analytical model (Equation 7), an experimental identification of the closed-loop system was performed.

System Identification

Due to open-loop instability, experimental models for the vehicle can be obtained through closed-loop experiments only (Fig. 7). In the procedure carried out, the first step was to design

Table 2. Data for each electromagnet	
Nominal air gap	$Z_0 = 0.005\,m$
Steady state current	$I_0 = 1.7124\,A$
Dimensions	$a = 0.03\,m\ c = 0.064\,m$
Number of turns	$N = 1300$
Air permeability	$\mu_0 = 4\pi 10^{-7}\,\frac{H}{m}$
Analogic power circuit gain	$k_{pc} = 0.001512\,\frac{m}{A}$
Mass of a quarter of vehicle	$m_e = \frac{M}{4} = 24.4\,kg$

Table 3. Gains k_p and $\bar{k}_p$ $(p = 1, \ldots, 4)$	
$k_1 = -0.28$	$\bar{k}_1 = 1.13$
$k_2 = -0.27$	$\bar{k}_2 = 1.14$
$k_3 = -0.25$	$\bar{k}_3 = 1.25$

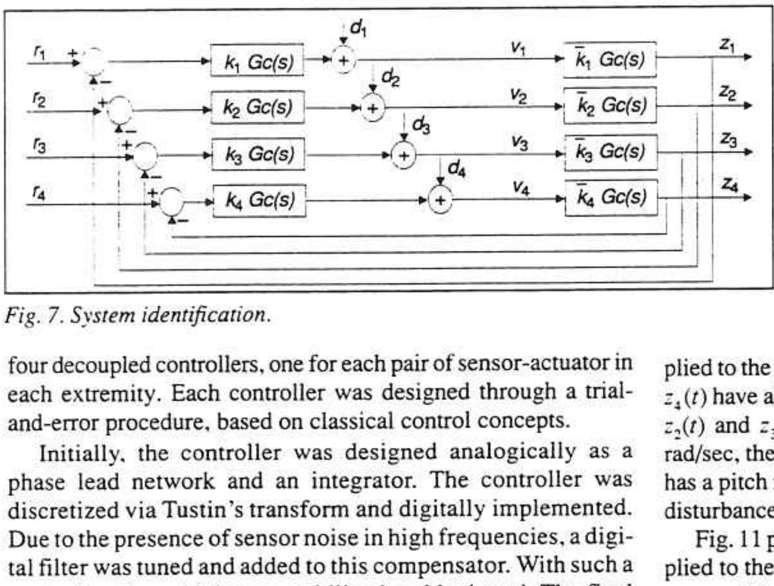

Fig. 7. System identification.

four decoupled controllers, one for each pair of sensor-actuator in each extremity. Each controller was designed through a trial-and-error procedure, based on classical control concepts.

Initially, the controller was designed analogically as a phase lead network and an integrator. The controller was discretized via Tustin's transform and digitally implemented. Due to the presence of sensor noise in high frequencies, a digital filter was tuned and added to this compensator. With such a controller, the vehicle was stabilized and levitated. The final continuous time version of the complete compensator $G_c(s)$ is given by

$$G_c(s) = \frac{k_p(s+0.8)(s+103)(s+126)(s \pm 7000)(s+7835)}{s(s+368)(s+340 \pm 179j)(s+7196 \pm 347j)}, \tag{8}$$

where k_p $(p = 1, \ldots, 4)$ are gains.

Some important features of the controller $G_c(s)$ are:

- Lead-lag phase characteristic
- Occurrence of phase lead in low frequencies. According to Fig. 8, the phase lead occurs approximately in the range from 10 to 400 rad/sec. This characteristic is essential to produce closed-loop stability, since the open-loop model (Equation 7) is unstable.
- Presence of high-frequency poles to reject sensor noise
- Presence of an integrator to obtain null steady-state error for step inputs at the reference and step disturbances at the plant input (load disturbances). System stabilization for gaps significantly different from the nominal one is difficult; large gaps require excessive electrical power, whereas small gaps lead to high electromagnet inductances, which make it difficult to produce fast control actions.

The second step was to measure the closed-loop frequency responses. Assuming that around the equilibrium point the vehicle behaves as a SISO system (Fig. 7), four closed-loop transfer functions

$$G_{clp}(s) = \frac{z_p(s)}{d_p(s)} \tag{9}$$

$(p = 1, \ldots, 4)$ were identified. For this identification, an HP 3562A Dynamic Signal Analyzer was employed to inject a sinusoidal signal d_p and to measure respective outputs z_p $(p = 1, \ldots, 4)$.

In Fig. 7, the gains k_p $(p = 1, \ldots, 4)$ represent adjusted gains due to constructive differences of the vehicle and power circuits. Such differences are represented by the gains $\bar{k}_p$ $(p = 1, \ldots, 4)$, which were determined through the comparison of the closed-loop frequency responses obtained from Equations 7 and 8 and the experimental ones. The model for the plant becomes, therefore, $G_p(s) = \bar{k}_p G(s)$, $(p = 1, \ldots, 4)$.

The final values of gains k_p and $\bar{k}_p$ are presented in Table 3.

The four analytical and experimental closed-loop frequency responses are presented in Fig. 9, which shows a fundamental resonance peak around $\omega = 10$ rad/sec.

Fig. 10 presents the system response for a sinusoidal disturbance of frequency $\omega = 10$ rad/sec applied to the plant output $z_2(t)$. It can be verified that gaps $z_1(t)$ and $z_4(t)$ have a phase difference of 180 degrees with respect to gaps $z_2(t)$ and $z_3(t)$, which leads to the conclusion that, for $\omega = 10$ rad/sec, the closed-loop system with the controller (Equation 8) has a pitch resonant frequency. The same conclusion is valid for disturbance signals applied to outputs $z_1(t)$, $z_3(t)$, and $z_4(t)$.

Fig. 11 presents the system response for a step disturbance applied to the plant output $z_1(t)$. The resonance peaks in Fig. 9 are responsible for the system oscillations presented in Fig. 11 and

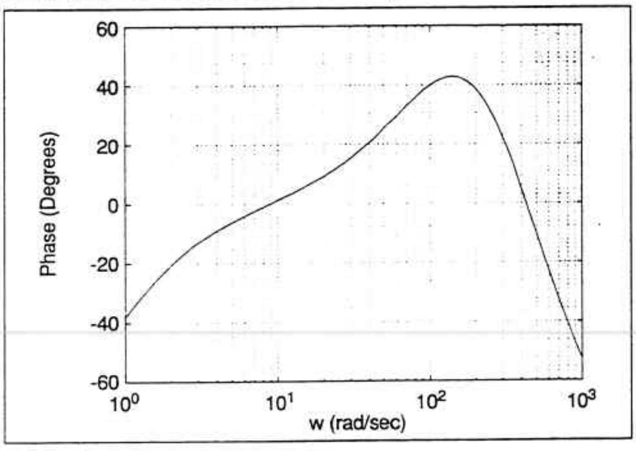

Fig. 8. Phase × frequency of $G_c(s)$.

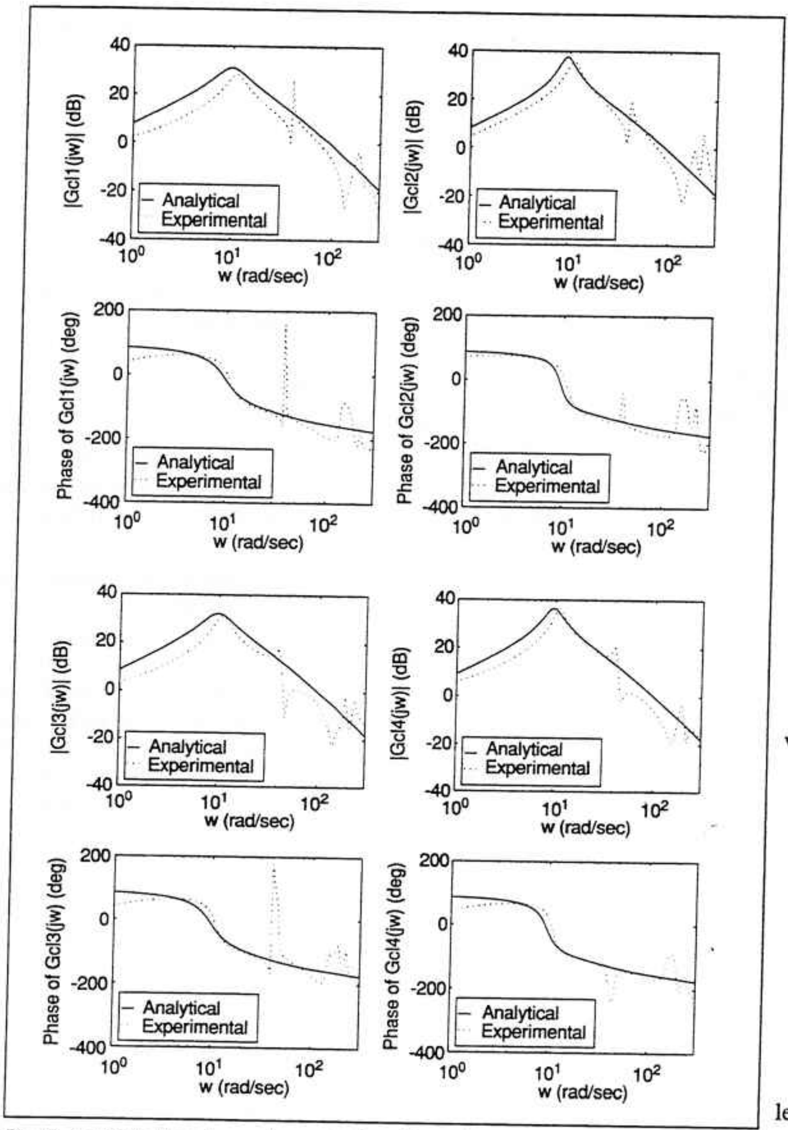

Fig. 9. Analytical and experimental closed-loop frequency responses.

represent the low damped pitch resonant frequency of the closed-loop system.

The main design requirement presented in the next section is to attenuate these resonance peaks through the H_2 and H_∞ control design techniques.

H_2 and H_∞ Control Designs

The design methodologies for H_2 and H_∞ control synthesis are described in [13]; briefly speaking, given the "augmented plant" $G_{ap}(s)$, as in Fig. 12, the design objective is to find a stabilizing controller $K(s)$, such that the norm of the closed-loop transfer function matrix

$$T_{y_1 r_1}(s) \triangleq \begin{bmatrix} W_1(s)S(s) \\ W_2(s)K(s)S(s) \\ W_3(s)T(s) \end{bmatrix} \qquad (10)$$

is small. $S(s)$ and $T(s)$ are the sensitivity and complementary sensitivity functions, respectively, given by

$$S(s) = \frac{1}{1+G_p(s)K(s)}; \quad T(s) = \frac{G_p(s)K(s)}{1+G_p(s)K(s)}.$$

The H_2 controller minimizes $\|T_{y_1 r_1}\|_2$ and the H_∞ controller makes $\|T_{y_1 r_1}\|_\infty < \gamma$, for a given γ.

Design Specifications

The design specifications are to:

- Attenuate the resonance peak at $\omega = 10$ rad/sec in Fig. 9
- Minimize the sensitivity function as much as possible. Since the sensitivity function is related to the low frequency gain, its minimization is also limited by the lowest possible gain due to the open-loop instability.
- Obtain -60 dB/decade roll-off above $\omega = 400$ rad/sec, due to sensor noise.

Criteria to Choose the Weighting Functions

In both cases, H_2 and H_∞, the weighting functions were chosen such that (see Fig. 13):

- W_3 determines an upper bound for the closed-loop resonance peak
- W_2 acts as an upper bound for the controller gain, being thus related to the closed loop robustness characteristics
- W_1 is related to the performance requirements, acting as a lower bound for the sensitivity function.

Transfer Functions

The transfer function obtained for the H_2 controller for electromagnet 1 is given by

$$K(s) = \frac{10205(s+0.8)(s+60.0)(s+62.6)(s+100.0)}{(s+0.001)(s+57.5)(s+72.5)(s+301.7 \pm 299.2j)}, \qquad (11)$$

with

$$W_1(s) = \frac{0.65}{s+0.001}, \quad W_2(s) = \frac{0.05(s+1)}{s+100},$$

and

$$W_3(s) = \frac{0.9(s+10)(s+20)}{(s+60)(s+100)}.$$

The transfer function obtained for the H_∞ controller for the electromagnet 1 is given by

$$K(s) = \frac{737.2(s+0.8)(s+62.6)(s+150)(s+200)(s+14000)}{(s+0.001)(s+74)(s+353)(s+216 \pm 280j)(s+11542)}, \qquad (12)$$

with

$$W_1(s) = \frac{0.35}{s + 0.001}, \quad W_2(s) = \frac{6(s+1)}{s + 14000},$$

$$W_3(s) = \frac{2(s+10)(s+20)}{(s+150)(s+200)}.$$

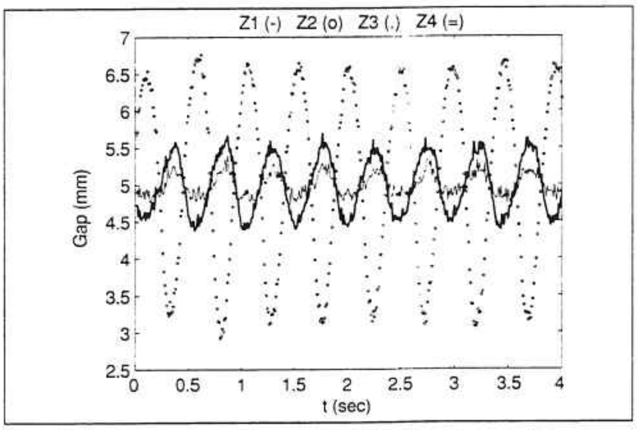

Fig. 10. System response for a sinusoidal disturbance of frequency 10 rad/sec applied to the plant output $z_2(t)$.

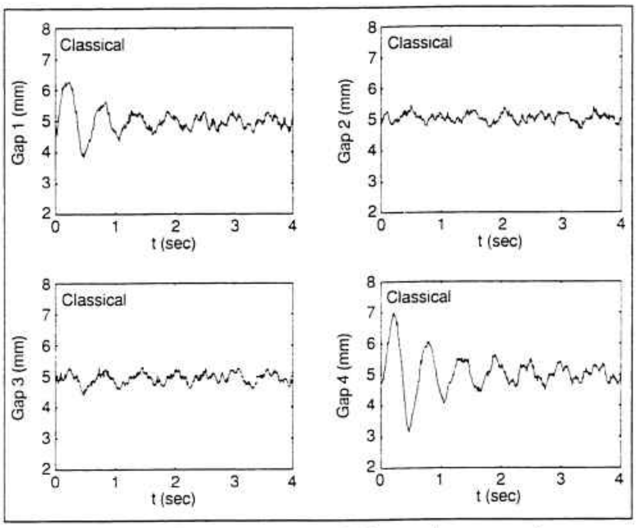

Fig. 11. Closed-loop response of the real system for a step disturbance applied to the plant output $z_1(t)$ with classical controller.

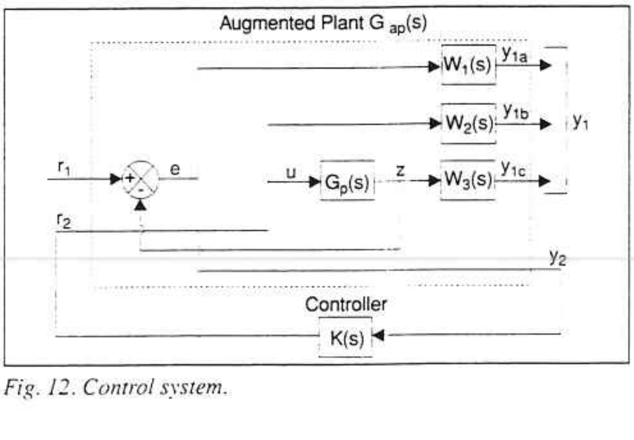

Fig. 12. Control system.

and $\gamma = \gamma_{min} \cong 0.3832$, where γ_{min} is the minimum positive value such that $\|T_{y1r1}\|_\infty < \gamma$.

The H_∞ norm of $T_{y1r1}(s)$, denoted $\|T_{y1r1}\|_\infty$, is defined as

$$\|T_{y1r1}\|_\infty \triangleq \sup_\omega \sigma_{max}[T_{y1r1}(j\omega)], \tag{13}$$

where $\sigma_{max}[T_{y1r1}(j\omega)]$ is the maximum singular value of $T_{y1r1}(j\omega)$.

In Fig. 14, it is shown that $\sigma_{max}[T_{y1r1}(j\omega)] < \gamma$ for $\omega \in [0.01 \quad 1000]$ with the controller (Equation 12).

Remarks

Several remarks are in order at this point.

- Although the weighting function W_3 is usually employed to shape the closed-loop transfer function at high frequencies, it is worth noting that in the present designs a different strategy was adopted, as mentioned previously.

  In addition to the usual design trade offs, the open-loop instability and nonlinear characteristic (Equation 2) impose a lower bound for the open-loop gain at low frequencies. In other words, the weighting function W_1, which was conceived as an approximated integrator, is also related to the minimum gain required to stabilize the closed-loop system. As a consequence, the tuning of the weighting function W_3 is limited by the specification of W_1, since the attenuation of the resonance peak implies, in general, in decreasing the low frequency gain.
- It can be observed that both H_2 and H_∞ controllers cancel the stable pole of the plant (Equation 7) at $s = -\sqrt{2g/Z_0} \cong -62.6$. Such cancellation results possibly from an undesirable plant $G_p(s)$, in face of specified closed-loop shapes. In other words, the controller $K(s)$, which appropriately shapes the open-loop $K(s)G_p(s)$, worked in this direction, inverting the stable dynamic of the plant. In the present designs, this fact does not represent any problem, since this pole is not related to a low damped resonance frequency.
- Although different weighting functions had been employed for the H_2 and H_∞ controller syntheses, the sensitivity and complementary sensitivity functions obtained with such controllers are very similar, as shown in Fig. 15. The weighting functions for both H_2 and H_∞ designs are the results of an iterative procedure. The design specifications in the way presented, as well as the different objectives between the H_2 and H_∞ frameworks (to minimize rms values and to flatten out $|G_p(jw)|$, respectively) may lead to different weighting functions in each case.
- The robustness features of the three designed controllers can be evaluated from the Nyquist criterion. As indicated in Table 4, in the neighborhood of the critical point (–1), only the inferior gain margins are relevant and indicate a higher robustness degree for the H_2 and H_∞ controllers when compared to the classical controller.

Experimental Results

The classical, H_2, and H_∞ controllers were implemented on a 200 MHz Pentium PC. The controllers were discretized via

Tustin's transform at the sample rate of 3,500 Hz. The data acquisition board consists of 12-bit A/D and 8-bit D/A converters.

Fig. 16 presents the closed-loop responses of the real system with the H_2 and H_∞ controllers for a reference gap of 5 mm. A step disturbance was applied to the plant output 1 by adding a constant to the measurement of the gap $z_1(t)$. This figure shows that the levitation system presents equivalent responses for the H_2 and H_∞ controllers. The closed-loop system is stable and has a nice transient response, and the step disturbance has been rejected completely in steady-state.

Furthermore, such responses are more damped and present smaller overshoots than the classical one (Fig. 11). This is in accordance with the smaller resonance peaks of the sensitivity functions (Fig. 15).

Another result is that the disturbance applied to the output $z_1(t)$ produces oscillations in the output $z_4(t)$ too, i.e., the vehicle tends to rotate around the angle θ.

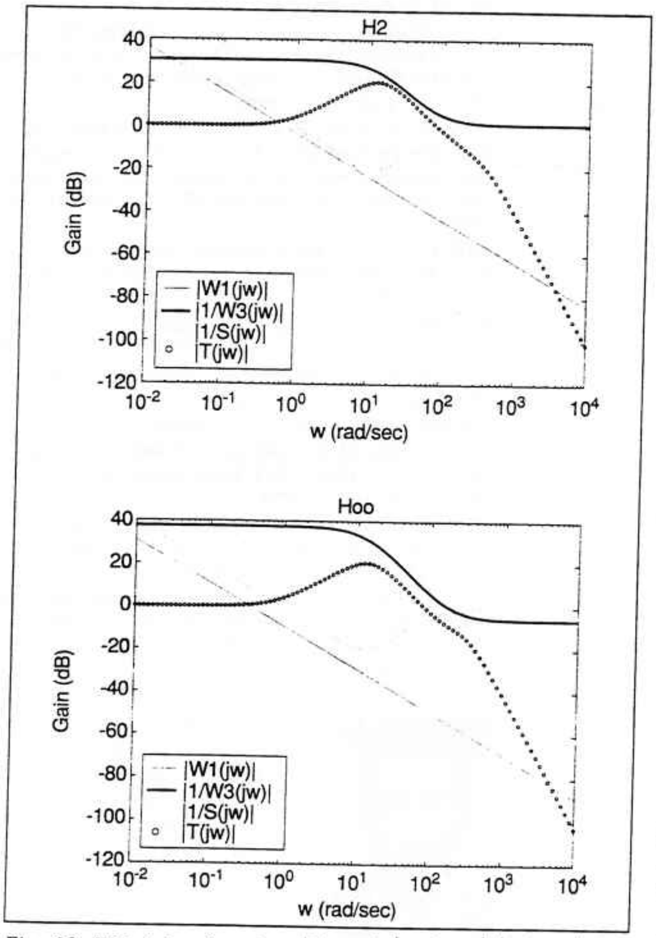

Fig. 13. Weighting functions $|W_1(jw)|$, $|W_3^{-1}(jw)|$, $|S^{-1}(jw)|$ *and* $|T(jw)|$.

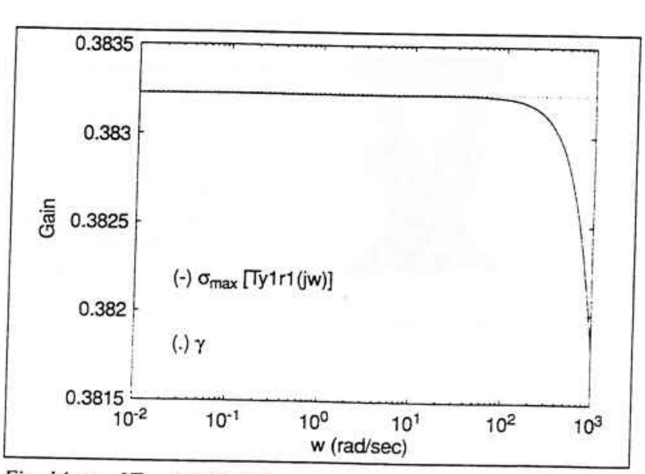

Fig. 14. $\sigma_{max}[T_{y1r1}(jw)] < \gamma$.

Conclusions and Future Research

This work presented an electromagnetically levitated vehicle prototype and a SISO analytical model linearized around an equilibrium point for the magnetic suspension system. Validation of this model was performed through closed-loop identification experiments. As the open-loop system is unstable, in order to perform such identification, the closed-loop system was first stabilized through a classical controller.

Table 4. Gain margins

Controller	Inferior Gain Margin (dB)	Superior Gain Margin (dB)
Classical	-0.5	19.0
H_2	-0.9	18.8
H_∞	-0.9	17.1

The identified closed-loop system presented a resonance peak around $\omega = 10$ rad/sec, which represents the pitch resonance. The attenuation of this resonance peak was obtained through a suitable weighting function W3 for the H_2 and H_∞ designs.

A step disturbance applied to the plant output showed that the responses with the H_2 and H_∞ controllers (Fig. 16) are very similar and present better performances when compared to the classical one (Fig. 11).

Comparing the H_2 and H_∞ controllers, it would be wrong to conclude from these designs which controller is better for this specific system. The results do not point to which controller is better but simply to the fact that the designs are similar.

Some suggestions for future research include: to test other control approaches in the levitation system; to measure other output signals, for example, the vertical acceleration of the vehicle; to add more electromagnets to the suspension system in order to evaluate the levitation system's robustness in the case of failures of actuators or sensors; to implement the propulsion system and to investigate the influence of movement on the levitation system; and to implement electromagnetically controlled lateral guides in the prototype.

References

[1] D. Rogg, "General survey of the possible applications and development tendencies of magnetic levitation technology," *IEEE Trans. Magn.*, vol. MAG-20, no. 5, pp. 1696–1701, 1984.

[2] S. Yamamura, S. Abe, and T. Hayashi, "Attractive electromagnet levitation of vehicles," *Elect. Eng. Japan*, vol. 94, no. 3, pp. 72–79, 1974.

[3] G. Bohn and G. Steinmetz, "The electromagnetic levitation and guidance technology of the TRANSRAPID test facility emsland," *IEEE Trans. Magn.*, vol. MAG-20, no. 5, pp. 1666–1671, 1984.

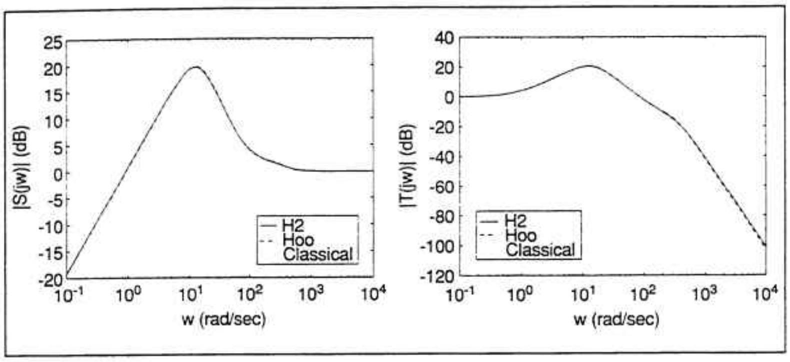

Fig. 15. Sensitivity and complementary sensitivity functions.

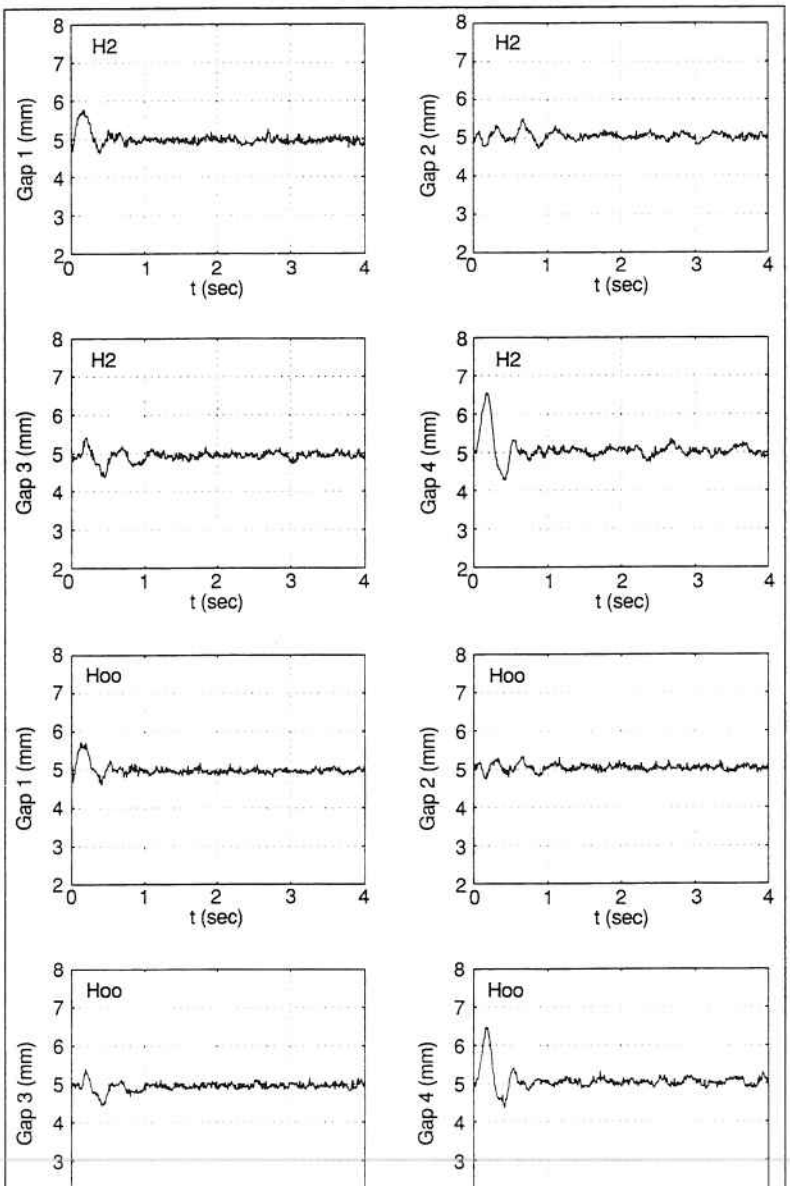

Fig. 16. Closed-loop responses of the real system for a step disturbance applied to the plant output $z_1(t)$ with H_2 and H_∞ controllers.

[4] E. Gottzein, R. Meisinger, and L. Miller, "The magnetic wheel in the suspension of high-speed ground transportation vehicles," *IEEE Trans. Veh. Technol.*, vol. VT-29, no. 1, pp. 17–22, 1980.

[5] K. Glatzel, G. Khurdok, and D. Rogg, "The development of the magnetically suspended transportation system in the Federal Republic of Germany," *IEEE Trans. Veh. Technol.*, vol. VT-29, no. 1, pp. 3–16, 1980.

[6] Y. Hikasa and Y. Takeuchi, "Detail and experimental results of ferromagnetic levitation system of Japan Air Lines HSST-01/-02 vehicles," *IEEE Trans. Veh. Technol.*, vol. VT-29, no. 1, pp. 35–41, 1980.

[7] B. V. Jayawant, P. K. Sinha, A. R. Wheeler, R. J. Whorlow, and J. Willsher, "Development of 1-ton magnetically suspended vehicle using controlled D.C. electromagnets," *Proc. Inst. Elect. Eng*, vol. 123, no. 9, pp. 941–948, 1976.

[8] B. V. Jayawant, "Electromagnetic suspension and levitation," *Proc. Inst. Elect. Eng.*, vol. 129, pt. A, no. 8, pp. 549–581, 1982.

[9] J. Meins, L. Miller, and W. J. Mayer, "The high speed MagLev transportation system TRANSRAPID," *IEEE Trans. Magn.*, vol. MAG-24, no. 2, pp. 808–811, 1988.

[10] P. K. Sinha, *Electromagnetic suspension: dynamics and control.* Stevenage, U.K.: Peregrinus, 1987.

[11] S. Suzuki, M. Kawashima, Y. Hosoda, and T. Tanida, "HSST-03 SYSTEM," *IEEE Trans. Magn.*, vol. MAG-20, no. 5, pp. 1675–1677, 1984.

[12] P. K. Sinha, "Design of a magnetically levitated vehicle," *IEEE Trans. Magn.*, vol. MAG-20, no. 5, pp. 1672–1674, 1984.

[13] J. C. Doyle, K. Glover, P. P. Khargonekar, and B. A. Francis, "State-space solutions to standard H_2 and H_∞ control problems," *IEEE Trans. Autom. Contr.*, vol. AC-34, pp. 831–847, 1989.

Anselmo Bittar was born in Sao Paulo, Brazil, in 1967. He received his B.Sc. And M.Sc. Degrees in electrical engineering from the University of Sao Paulo (USP) in 1990 and 1993, respectively. He is working toward his doctoral degree in systems engineering at the USP Department of Electronic Engineering. His dissertation work consists of developing control systems for an electromagnetically levitated vehicle prototype. His research interests include magnetic levitation, magnetic bearings, and robust control design.

Roberto Moura Sales was born in Sao Paulo, Brazil, in 1952. He received his M.Sc. and doctoral degrees in systems engineering from USP in 1981 and 1984, respectively. He is professor of electrical engineering and coordinator of the Laboratory of Automation and Control at the USP Department of Electronic Engineering. His research interests include magnetic levitation, H_2 and H_∞ control, and optimization.

BOLETINS TÉCNICOS - TEXTOS PUBLICADOS

BT/PEE/9301 - Oscilador a HEMT - 10 GHz - FÁTIMA S. CORRERA, EDMAR CAMARGO

T/PEE/9302 - Representação Senoidal da Voz através dos Polos do Filtro Preditor - MARCELO B. JOAQUIM, NORMONDS ALENS

BT/PEE/9303 - Blindagens por Grades Condutoras: Cálculo do Campo Próximo - LUIZ CEZAR TRINTINALIA, ANTONIO ROBERTO PANICALI

BT/PEE/9304 - Sistema de Otimização e Controle de Produção em Minas de Pequeno e Médio Porte - TSEN CHUNG KANG, VITOR MARQUES PINTO LEITE

BT/PEE/9401 - Determinação das Frases de Aplicação Forense para o projeto NESPER e Tese de Mestrado IME/94, com Base em Estudos Fonéticos - MARCONI DOS REIS BEZERRA, EUVALDO F. CABRAL JUNIOR

BT/PEE/9402 - Implementação e Teste de uma Rede Neural Artificial do TIpo KSON (Kohonen Self-Organizing Network) com Entradas Bidimensionais - MARCELO YASSUNORI MATUDA, EUVALDO F. CABRAL JR.

BT/PEE/9403 - Transformada de Walsh e Haar Aplicadas no Processamento de Voz - ALEXANDRE AUGUSTO OTTATI NOGUEIRA, THIAGO ANTONIO GRANDI DE TOLOSA, EUVALDO F. CABRAL JÚNIOR

BT/PEE/9404 - Aplicação de Redes Neurais ao Problema de Reconhecimento de Padrões por um Sonar Ativo - ALEXANDRE RIBEIRO MORRONE, CRISTINA COELHO DE ABREU, EDUARDO KOITI KIUKAWA, EUVALDO F. CABRAL JR.

BT/PEE/9405 - Tudo que se Precisa Saber sobre a Prática da FFT - Transformada Rápida de Fourier (Inclui Software) - ROGÉRIO CASAGRANDE, EUVALDO F. CABRAL JR.

BT/PEE/9406 - A Survey on Speech Enhancement Techniques of Interest to Speaker Recognition - CELSO S. KURASHIMA, EUVALDO F. CABRAL JR.

BT/PEE/9407 - Identificação de Pulsos Decádicos em Linhas Telefônicas - ANTONIO P. TIMOSZCZUK, MÁRCIO A. MATHIAS, EUVALDO F. CABRAL JR.

BT/PEE/9408 - Implementação e Teste de Filtros do Tipo Adaptativo e ©Notchª para a Remoção de Interferência de 60 Hz em Sinais de Eletrocardiograma - FLÁVIO ANTÔNIO MENEGOLA, JOSÉ AUGUSTO DE MATTOS, JOSÉ GOMES G. FILHO, SIDNEY SILVA VIANA, EUVALDO F. CABRAL JR.

BT/PEE/9409 - Compressão de Sinais de Voz utilizando Transformadas de Karhunen-Loève, Fourier e Hadamard - IVAN LUIS VIEIRA, LUIZ FERNANDO STEIN WETZEL, EUVALDO F. CABRAL JR.

BT/PEE/9410 - ©Ray Tracingª Paralelo - EDUARDO TOLEDO SANTOS, JOÃO ANTONIO ZUFFO

BT/PEE/9411 - Implementação de uma Ferramenta Posicionador para ©Gate-Arraysª Tipo Mar de Portas - JORGE W. PERLAZA PRADO, WILHELMUS A. M. VAN NOIJE

BT/PEE/9412 - Tudo que se Precisa Saber Sobre a Teoria da FFT - Transformada Rápida de Fourier - FÁBIO LUÍS ROMÃO, REINALDO SILVEIRA, ROGÉRIO CASAGRANDE, EUVALDO CABRAL JR.

BT/PEE/9413 - Análise do Ruído Sonoro em uma Sala de Aquisição de Amostras de Som com Microcomputador - FÁBIO LUÍS ROMÃO, REINALDO SILVEIRA, EUVALDO CABRAL JR.

BT/PEE/9414 - Cor: Aspectos Relevantes para Visualização de Dados - SÍLVIA DELGADO OLABARRIAGA

BT/PEE/9415 - Projeto de Filtros Digitais IIR com Fase Aproximadamente Linear Utilizando Redução de Ordem - IVAN F. J. RODRIGUES, MAX GERKEN

BT/PEE/9416 - GERAFILTRO: Sistema para Projeto Automático de Filtros Digitais ©IIRª (da especificação em alto nível ao leiaute do ©ASICª) - RICARDO PIRES, JOSÉ VIEIRA DO VALE NETO

BT/PEE/9417 - Redes Neurais Artificiais Aplicadas à Identificação de Pulsos Decádicos em Linhas Telefônicas - ANTONIO P. TIMOSZCZUK, EUVALDO F. CABRAL JR.

BT/PEE/9501 - Estudo Comparativo de Métodos de Cálculo da Frequência Fundamental - MARCOS COSTA HUNOLD, EUVALDO F. CABRAL JR.

BT/PEE/9502 - Combinando Técnicas de Redes Neurais Artificiais e Informações de Excitação no Reconhecimento Automático do Locutor - ANDRÉ BORDIN MAGNI, EUVALDO F. CABRAL JR.

BT/PEE/9503 - Utilização de Redes Neurais Artificiais para Detecção e Identificação de Falhas em Circuitos - MÁRCIO YUKIO TERUYA, ROBERTO AMILTON BERNARDES SÓRIA, EUVALDO CABRAL JR.

BT/PEE/9504 - Uso de Redes Neurais Artiificiais no Reconhecimento de Locutores no Domínio Temporal - BENEDITO JOSÉ BARRETO FONSECA JÚNIOR, EUVALDO CABRAL JÚNIOR

BT/PEE/9505 - Projeto de Filtros Passivos e Ativos em Técnicas de Circuitos Integrados de Microondas - DAVID VIVEIROS JÚNIOR, DENISE CONSONNI

BT/PEE/9506 - Uma Análise de Clustering para as Frases de Projeto NESPER - RONALDO OLIVEIRA MESSINA, EUVALDO F. CABRAL JR.

BT/PEE/9507 - Controle com Estrutura Variável e Modos Deslizantes - Um Estudo para Aplicação em Controle Carga-frequência da Geração - JOSE PAULO F. GARCIA, JOCELYN FREITAS BENNATON

BT/PEE/9508 - Recuperação das Margens de Ganho e de Fase para Sistemas de Fase Não Mínima por Realimentação da Saída - MARCO H. TERRA, VITOR M. P. LEITE

BT/PEE/9509 - Sistema de Inspeção Óptica de Dispositivos Bi-Dimensionais - CASIMIRO DE ALMEIDA BARRETO, PEDRO LUÍS PRÓSPERO SANCHEZ

T/PEE/9510 - Sistema de Partículas Uma Poderosa Técnica de Animação em Computação Gráfica - RENATO CURTO RODRIGUES, JOÃO ANTÔNIO ZUFFO

BT/PEE/9511- Efeito de Ruídos em Sinais de Voz Visualizados em Trajetórias Neurais de Kohonen - CELSO S. KURASHIMA, EUVALDO F. CABRAL JR.

BT/PEE/9601 - "Um Reconhecedor de Sinais Sonoros Utilizando LVQ" - ALEXANDRE TORNICE, EUVALDO CABRAL JR.

BT/PEE/9602 - "Coleção Artificial Neural Networks: Uma Visão Geral dos Sistemas Neurais Artificais de Stephen Grossberg" - CHIU HSIUNG HUANG

BT/PEE/9603 - "Reactively-Sputtered TiN Formation Using a RF Magnetron System"- SÉRGIO PAULO AMARAL OSÓRIO, LUIZ SÉRGIO ZASNICOFF

BT/PEE/9604 - Aspectos em Tradução de Linguagens Naturais Através de Redes Neurais Artificiais - CARLOS EDUARDO DANTAS DE MENEZES, EUVALDO F. CABRAL JR.

BT/PEE/9605 - Implementação de Blocos Passa-Tudo Utilizando Realimentação de Erro - SÉRGIO JOSÉ CARNEIRO LEÃO, MAX GERKEN

BT/PEE/9606 - Coleção SANN group Redes Neurais Artificiais: A Rede Neural de Sakoe - ANDRÉ BORDIN MAGNI, EUVALDO F. CABRAL JR.

BT/PEE/9607 - Coleção SANN group Redes Neurais Artificiais: A Rede Neural de Steinbuch - ROBERTO AMILTON BERNARDES SÓRIA, EUVALDO F. CABRAL JR.

BT/PEE/9608 - Desenvolvimento de uma Estrutura de Duplo Nível de Metal para a Confecção de Interconexões em Circuitos Integrados - JOSÉ AUGUSTO DE ALENCAR PEREIRA, LUIZ CARLOS MOLINA TORRES

BT/PEE/9609 - Determinação de Parâmetros de Processo para Fotomáscara "Balzers" Utilizando Gerador de Padrões - JORGE SEKI, MEGUMI SAITO

BT/PEE/9610 - Um Ambiente para Desenvolvimento de Sistemas Distribuídos - PEDRO F. ROSA, JOÃO A. ZUFFO

BT/PEE/9611 - Interpretações Teóricas do Funcionamento Cerebelar: Uma Revisão - MARCUS FRAGA VIEIRA, ANDRÉ FÁBIO KOHN

BT/PEE/9612 - Marcapasso Cardíaco Temporário Microcontrolado de Demanda e Baixo Consumo - FLAVIO ANTONIO MENEGOLA, JOSÉ CARLOS TEIXEIRA DE BARROS MORAES

BT/PEE/9613 - Um Sistema de Planejamento de Ação Baseado em Casos para uma Célula Flexível de Manufatura - RICARDO LUÍS DE FREITAS, MÁRCIO RILLO

BT/PEE/9614 - Aplicações do Boundary-Scan para o Teste de Módulos Multichip - ROBERTO C. COSSI JR., JOSÉ ROBERTO DE A. AMAZONAS

BT/PEE/9615 - A 2.488 Gb/s GaAs 1:4/1:16 Demultiplexer IC with Skip Circuit for Sonet STS-12/48 Systems - TAUFIK ABRÃO, FATIMA S. CORRERA

BT/PEE/9616 - Uma Contribuição para a Construção de Algoritmos em Projetos de Redes - ALLAN DE SOUZA, JOSÉ ROBERTO CASTILHO PIQUEIRA

BT/PEE/9617 - Análise Crítica dos Métodos de Medição do Intervalo QT do Eletrocardiograma - SÍDNEY DA SILVA VIANA, JOSÉ CARLOS TEIXEIRA DE BARROS MORAES

BT/PEE/9618 - Deposição e Caracterização de Filmes de SiO2 Crescidos pela Técnica de PECVD a Baixa Temperatura - MARCO ALAYO CHÁVEZ, INÉS PEREYRA

BT/PEE/9619 - PARSTOOL: Uma Ferramenta de Auxílio à Simulação de Sistemas Paralelos - LI KUAN CHING, LIRIA MATSUMOTO SATO

BT/PEE/9620 - Análise de um Método de Otimização por Malha no Treinamento de Robôs - OLÍMPIO MURILO CAPELI, JOSÉ CARLOS T. B. MORAES, SADAO ISOTANI

BT/PEE/9701 - Identification of Unstable Mechanical Systems - ROBERTO MOURA SALES, ANSELMO BITTAR, MICHAEL PORSCH, LAÉRCIO LUCCHESI

BT/PEE/9702 - Analysis of the Subthreshold Slope Transition Region in SOI nMOSFET - VICTOR SONNENBERG, JOÃO ANTONIO MARTINO

BT/PEE/9703 - Introduction of the SOI MOSFET Dimensions in the High-Temperature Leakage Drain Current Model - MARCELO BELLODI, JOÃO ANTONIO MARTINO, DENIS FLANDRE

BT/PEE/9704 - Controle de Largura de Banda Dinâmica para Transmissões Multicast para Redes de Alta Velocidade - SANG SOON LEE, SERGIO TAKEO KOFUJI

BT/PEE/9705 - Uma Modificação Proposta para o Controle Preditivo Generalizado com Filtro de Kalman - JAIME QUINTERO R., OSWALDO L. V. COSTA

BT/PEE/9706 - Aplicações de Redes Neurais em Previsões Financeiras - OLÍMPIO MURILO CAPELI, EUVALDO F. CABRAL JR.

BT/PEE/9707 - Sistema Microcontrolado, Multicanal e Portátil para Estimulação Neuromuscular Funcional - ROGÉRIO QUIARIM ZARZA, JOSÉ CARLOS TEIXEIRA DE BARROS MORAES

BT/PEE/9708 - Requisitos para o Mapeamento Tecnológico em Projetos de Microeletrônica - LUCIANO DE OLIVEIRA CORRÊA DE BRITO, JOSÉ ROBERTO DE ALMEIDA AMAZONAS

BT/PEE/9709 - Sistemas PRMA com Dados Acoplados - JOSÉ AUGUSTO DE LIMA, PAUL JEAN ETIENNE JESZENSKY

BT/PEE/9710 - Algoritmos Genéticos (AG's) para a Otimização de Controladores Nebulosos - JULIO CESAR CEBALLOS AYA, OSWALDO L. V. COSTA

BT/PEE/9711 - Um Estudo Sobre a Redução de Ruídos em Sinais Caóticos - ERNANE JOSÉ XAVIER COSTA, EUVALDO F. CABRAL JR.

BT/PEE/9712 - Geradores não Lineares de Sequência para uso em Sistemas Spread Spectrum - ANGEL ANTONIO GONZALEZ MARTINEZ, PAUL JEAN ETIENNE JESZENSZKY

BT/PEE/9713 - Modelamento Físico do Sistema Heteroestrutura - Metal - CECÍLIA WETTERLE RODRIGUES, MEGUMI SAITO

BT/PEE/9714 - Tensões Induzidas em Linhas Aéreas por Descargas Atmosféricas Indiretas - Modelagem e Aplicação ao Cálculo de Interrupções - ALEXANDRE PIANTINI, JORGE M. JANISZEWSKI

BT/PEE/9715 - RECMAP - Uma Ferramenta para Otimização em Síntese de Alto Nível Baseada em Reconhecimento Funcional e Mapeamento de Componentes - ANDRÉ GERHARD, JOSÉ VIEIRA DO VALE NETO

BT/PEE/9716 - Estudo da Sinterização de Contatos Al/Ti por Recozimento Térmico Rápido Visando a Aplicação em Circuitos Integrados - ANGELO EDUARDO BATTISTINI MARQUES, ROGÉRIO FURLAN

BT/PEE/9717 - Mixed H2/H- Control of Discrete-Time Markovian Jump Linear Systems - OSWALDO L. V. COSTA, RICARDO P. MARQUES

BT/PEE/9718 - Aluminium Etching with CCl4-N2 Plasmas - ANGELA MAKIE MAKAZAWA, PATRICK VERDONCK

BT/PEE/9719 - O Uso de Resistes Amplificados Quimicamente e de Sililação em Litrografia por Feixe de Elétrons - ANTONIO C. SEABRA, PATRICK B. VERDONCK

BT/PEE/9720 - Implementação de um Simulador de um Circuito Neuro-Medular que Atua no Controle da Força Motora - LUIZ JURANDIR SIMÕES DE ARAÚJO,ANDRÉ FÁBIO KOHN

BT/PEE/9721 - Avaliação das Características Físico-Químicas e Elétricas de Filmes de SiO2 Depositados por PECVD a Patir da Reação entre O2 e TEOS - ALVARO ROMANELLI CARDOSO E CLAUS MARTIN HASENACK

BT/PEE/9722 - Controle e Simulação Dinâmica de Colunas de Destilação: Aplicação Prática em uma Coluna com Refluxo por Gravidade

BT/PEE/9723 - Circuitos de Portas Lógicas Primitivas Implementados a Partir de uma Classe de Lógicas Paraconsistentes Anotadas - JOÃO INÁCIO DA SILVA FILHO, JAIR MINORO ABE, PEDRO LUÍS PRÓSPERO SANCHEZ

BT/PEE/9724 - Lattice Heating and Energy Balance Consideration on the I-V Characteristics of Submicrometer Thin-Film Fully Depleted SOI NMOS Devices - CLAUDIA BRUNETTI, NELSON L. A. BRAGA, LUIZ S. ZASNICOFF

BT/PEE/9725 - Identificação de um Processo de Neutralização de pH via Redes Neurais - SILVIO FLABOREA, CLAUDIO GARCIA

BT/PEE/9726 - Uma Estratégia de Migração de Sistemas de Telefonia Movél com Tecnologia AMPS para a Tecnologia CDMA - RONALD LUÍS CLARKSON EISNER, PAUL JEAN ETIENNE JESZENSKY

BT/PEE/9727 - Controle de pH Usando Conceitos de Invariantes de Reações e Geometria Diferencial - OSCAR A. ZANABARIA S., CLAUDIO GARCIA

BT/PEE/9728 - Estudo da Influência dos Parâmetros de Recozimento Térmico Rápido na Morfologia dos Filmes de TiSi2 Formados e sua Correlação com a Tensão Mecânica - SILVANA GASPAROTTO DE SOUZA, ARMANDO ANTONIO MARIA LAGANÁ, SEBASTIÃO GOMES DOS SANTOS FILHO

BT/PEE/9729 - Analysis of Silicon Surface Microirregularities by LASER Ligght Scattering - JOSÉ CÂNDIDO DE SOUSA FILHO, SEBASTIÃO GOMES DOS SANTOS FILHO

BT/PEE/9730 - Wavelets in Music Analysis and Synthesis: Timbres Analysis and Perspectives - REGIS ROSSI ALVES FARIA, RUGGERO ANDREA RUSCHIONI, JOÃO ANTONIO ZUFFO

BT/PEE/9731 - Estudo de Efeitos Mútuos da Distribuição de Corrente em Condutores - AUGUSTO CARLOS PAVÃO, JORGE MIECZYSLAW JANISZEWSKI

BT/PEE/9801 - Equivalência entre a Semântica da Lógica de Transações e a Semântica de sua Implementação Prolog - PAULO E. SANTOS, FLÁVIO S. C. DA SILVA

BT/PEE/9802 - Nash Game in Mixed H2/Hoo Control Theory a Convex Optimization Approach- HELENICE OLIVEIRA FLORENTINO, ROBERTO MOURA SALES

BT/PEE/9803 - Text-Independent Speaker Recognition Using Vector Quantization and Gaussian Mixture Models - THOMAS E. FILGUEIRAS Fº., RONALDO O. MESSINA E EUVALDO F. CABRAL JR.

BT/PEE/9804 - Elementos Piezoresistivos para Sensores de Pressão com Tecnologia CMOS - LUIZ ANTONIO RASIA, E. C. RODRIGUEZ

BT/PEE/9805 - Automação do Processo de Casamento de Impedância em Sistemas de Aquecimento por Microondas - J. C. DE SOUZA, J. T. SENISE, V. C. PARRO, F. M. PAIT

BT/PEE/9806 - Considerações para o Projeto de Células de Memória SI com Transistores HEMT - JAIME H. LASSO, EDGAR CHARRY R.

BT/PEE/9807 - Covariance Controller with Structure Constraint and Closed Loop H Bound - ANTÔNIO CARLOS DE LIMA, ROBERTO MOURA SALES

BT/PEE/9808 - Controle Unidimensional de Objetos: Uma Aplicação Prática em Fresadora Automática - MÁRCIO A. F. MURATORE, OSWALDO L. V. COSTA

BT/PEE/9809 - Redes Neurais com Retardos Temporais Aplicadas ao Reconhecimento Automático do Locutor - ROGÉRIO CASAGRANDE, EUVALDO F. CABRAL JR.

BT/PEE/9810 - Topological Computation and Voluntary Control - HENRIQUE SCHÜTZER DEL NERO, JOSÉ ROBERTO CASTILHO PIQUEIRA, ALFREDO PORTINARI MARANCA

BT/PEE/9811 - Casamento de Impedância em Guia de Onda Retangular Utilizando como Variável Medida a Potência Refletida - J. C. DE SOUZA JR., J. T. SENISE

BT/PEE/9812 - Applied Surface Science - RONALDO D. MANSANO, PATRICK VERDONCK, HOMERO S. MACIEL

BT/PEE/9813 - Contribuição ao Estudo da Morfologia da Superfície e da Interface do Siliceto de Titânio Formado sobre Si (100) Empregando a Técnica de Microscopia de Força Atômica (AFM) - N. M. HASAN, A. A. M. LAGANÁ, S. G. SANTOS FILHO

BT/PEE/9814 - Estudo Experimental da Tensão Mecânica em Filmes Finos de Cobre Obtidos por Evaporação ou Deposição Eletroquímica Espontânea - A. I. HASHIMOTO, S. G. FILHO

BT/PEE/9815 - Controle Híbrido de Manipuladores Robóticos - WEBER ALLEGRINI, JOSÉ JAIME DA CRUZ

BT/PEE/9816 - Entropia Informacional e Cronobiologia - ANA AMÉLIA BENEDITO SILVA, JOSÉ ROBERTO CASTILHO PIQUEIRA

BT/PEE/9817 - Estabilidade de Lyapunov e Controle de Atitude - FERNANDO SOUSA, FREITAS JÚNIOR, PAULO SÉRGIO PEREIRA DA SILVA

BT/PEE/9818 - Projeto de um Conversor de Frequências Resistivo em Tecnologia MMIC - CLÁUDIA C. A. APARÍCIO, DENISE CONSONNI

BT/PEE/9819 - Estudo de Sensibilidade de um Sistema de Modulação Digital via Simulação - RONALDO DI MAURO, LUIZ ANTONIO BACCALÁ

BT/PEE/9820 - Engenharia do Conhecimento Aplicada ao Conhecimento Aplicada ao Domínio de Gerenciamento de Falhas em Redes de Comunicação: Uma Abordagem Baseada em Modelo - MARILZA ANTUNES DE LEMOS, MARCIO RILLO

BT/PEE/9821 - Uma Biblioteca de Métodos de Resolução de Problemas de Planejamento para Fornecer Apoio à Aquisição de Conhecimento - LELIANE NUNES DE BARROS, MARCIO RILLO

BT/PEE/9822 - Um Estudo de Técnicas de Aprendizado por Reforço Livre de Modelo - Aplicação ao Pêndulo Invertido - SÉRGIO RIBEIRO AUGUSTO, ADEMAR FERREIRA

BT/PEE/9823 - Identificação de Sistemas Dinâmicos com Redes Neurais - FRANCISCO CARLOS PONS, CLÁUDIO GARCIA

BT/PEE/9824 - Comparison between Single and Double Langmuir Probe Techniques for Analysis of Inductively Coupled Plamas - RAUL M. DE CASTRO, GIUSEPPE A. CIRINO, PATRICK VERDONCK, HOMERO S. MACIEL, MARCOS MASSI, MARCELO B. PISANI, RONALDO D. MANSANO

BT/PEE/9825 - DECMEF: Um Sistema de Decomposição Aplicada à Síntese de Máquinas de Estados Finitos - CARLOS HUMBERTO LLANOS QUINTERO, MARIUS STRUM

BT/PEE/9826 - Controladores Preditivos Através de Desigualdade Matriciais Lineares - RENATO C. BARÃO, RICARDO P. MARQUES, OSWALDO L. V. COSTA

BT/PEE/9827 - Parametrization of all H2 Optimal Output Feedback Controllers - JOÃO YOSHIYUKI ISHIHARA, ROBERTO MOURA SALES

BT/PEE/9901 – Digital Equalization Using Time Delay Neural Network (TDNN) – MARIO ANDRÉS VERGARA ESCOBAR, EUVALDO F. CABRAL JR.

BT/PEE/9902 – Simulação e Análise Estrutural do Modelo de Deposição da Publicação ICRP 66 – JOAQUIM CARLOS SANCHES CARDOSO, JOSÉ CARLOS T. DE BARROS MOARAES

BT/PEE/9903 – Modelamento e Ajuste por Regra Sub-Ótica de Maximização da Informação da Mútua de um Sistema Reconhecedor de Palavras Isoladas, Independente do Falante, para Ambientes Adversos, com Redundância de Informação – MÁRIO MINAMI, IVANDRO SANCHES

BT/PEE/9904 – Modelagem Matemática e Controle Multivariável do Tanque de Contato Empregado no Processo de Lixiviação dos Minerais Niquelíferos – DANIEL GUZMÁN DEL RÍO, CLAUDIO GARCIA

BT/PEE/9905 – Avaliação de Transdutores para Análise Metabólica Humana – HENRIQUE TAKACHI MORIYA, JOSÉ CARLOS T. DE BARROS MORAES

BT/PEE/9906 – Estudo da Aplicação do Método TLM-2D à Análise de Campos Eletromagnéticos - MARCO ANTONIO MATHIAS, JORGE M. JANISZEWSKI

BT/PEE/9907 – Comportamento Transitório de Campos Eletromagnéticos em Meios Condutores: Simulação Computacional Eficiente por Diferenças Finitas no Domínio do Tempo – ALEXANDRE AUGUSTO OTTATI NOGUEIRA, JORGE MIECZYSLAW JANISZEWSKI